



Universiteit
Leiden
The Netherlands

High-pressure operando STM studies giving insight in CO oxidation and NO reduction of Pt(110)

Spronsen, M.A. van; Baarle, G.J.C. van; Herbschleb, C.T.; Frenken, J.W.M.; Groot, I.M.N.

Citation

Spronsen, M. A. van, Baarle, G. J. C. van, Herbschleb, C. T., Frenken, J. W. M., & Groot, I. M. N. (2015). High-pressure operando STM studies giving insight in CO oxidation and NO reduction of Pt(110). *Catalysis Today*, 244, 85-95. doi:10.1016/j.cattod.2014.07.008

Version: Publisher's Version

License: [Leiden University Non-exclusive license](#)

Downloaded from: <https://hdl.handle.net/1887/3194037>

Note: To cite this publication please use the final published version (if applicable).



High-pressure *operando* STM studies giving insight in CO oxidation and NO reduction over Pt(1 1 0)



M.A. van Spronsen*, G.J.C. van Baarle, C.T. Herbschleb, J.W.M. Frenken, I.M.N. Groot

Huygens-Kamerlingh Onnes Laboratory, Leiden University, P.O. Box 9504, 2300 RA Leiden, The Netherlands

ARTICLE INFO

Article history:

Received 1 June 2014

Accepted 7 July 2014

Available online 31 August 2014

Keywords:

CO oxidation

NO reduction

Platinum

Pt(1 1 0)

Surface reconstruction

Surface oxide

Operando

In situ

Scanning tunneling microscopy

ABSTRACT

Two catalytic systems have been studied at high pressures on the Pt(1 1 0) surface on an atomic level. The first system was the oxidation of CO by O₂ towards CO₂. In the framework of the second reaction, namely NO reduction, the effect of room temperature exposure of the surface to NO and H₂ was investigated. To study these reaction systems at relevant pressures, the ReactorSTM has been used. This is a unique system which consists of a compact STM in which a flow reactor is integrated. The combined reactor with STM is housed inside a conventional vacuum system to allow for traditional surface science preparation and analysis techniques. The STM images obtained with the ReactorSTM under reaction conditions show the lifting of the (1x2) missing row reconstruction by high-pressure CO exposure. The lifting is followed by the formation of the (1x1) metallic Pt(1 1 0) structure for high CO/O₂ ratios and a (1x2) lifted-row type surface oxide structure for more O₂-rich conditions. The room temperature exposure of Pt(1 1 0) to H₂ results in the formation of a (1x4) missing-row structure and deeper, nested missing rows. The exposure to high-pressure NO removes these missing-row structures.

© 2014 The Authors. Published by Elsevier B.V. This is an open access article under the CC BY-NC-SA license (<http://creativecommons.org/licenses/by-nc-sa/3.0/>).

1. Introduction

Much of our current knowledge of the precise mechanisms underlying chemical reactions at catalyst surfaces is derived from experiments under ultra-high vacuum (UHV) or high vacuum (HV) conditions. This discrepancy with respect to the typical working conditions of practical catalysts (*i.e.*, high pressures (HP) and elevated temperatures) comes from the fact that many surface-sensitive techniques such as low-energy electron diffraction (LEED), Auger electron spectroscopy (AES), and X-ray photoelectron spectroscopy (XPS) cannot be combined easily with the environment to which a catalyst would normally be exposed. Typical examples of catalysis would be the three-way catalyst in an automotive exhaust system, or catalytic processes in the petrochemical industry. Moreover, UHV conditions provide a clean and easily controllable environment for accurate experiments [1,2]. Although such low-pressure model studies have contributed extensively to our fundamental understanding of catalysts, recent investigations at high gas pressures have yielded new insights that go beyond the mere extrapolation of the low-pressure results [3–6]. This difference is often referred to as the “pressure gap” [7,8]. Recently, several

surface analysis techniques have been adapted to realistic conditions. Examples are transmission electron microscopy (TEM) [9], surface X-ray diffraction (SXRD) [10], scanning tunneling microscopy (STM) [8,11,12], and atomic force microscopy (AFM) [13].

Scanning tunneling microscopy is one of the few atomically sensitive surface science techniques that do not introduce fundamental problems or limitations when bridging the pressure gap. This technique can operate in the full range from UHV to HP of, *e.g.*, 1 bar and beyond, and from cryogenic temperatures to temperatures well above 1000 K [14,15]. With its capability to image surfaces with atomic resolution, STM holds the promise to determine the detailed dependence of the structure of model catalyst surfaces on various gas environments, to identify the active sites for catalytic reactions, and to elucidate the role of possible promoters, all under the relevant, high-pressure, high-temperature conditions of the catalytic processes of interest. The weak, local interaction of the tip with the surface provides confidence that in most cases this interaction will not significantly affect the structure and the properties of the catalyst. These advantageous properties of the technique go hand-in-hand with a demanding combination of technical difficulties, involving, *e.g.*, the imaging stability of the instrument in terms of drift and noise resulting from temperature and pressure variations, and from the presence of a gas flow. In addition, the signal-to-noise ratio in the detection of the reaction products in the gas mixture is demanding as well.

* Corresponding author. Tel.: +31 71 527 8407.

E-mail address: spronsen@physics.leidenuniv.nl (M.A. van Spronsen).

In order to investigate the relationship between surface structure and activity of a catalyst under industrially relevant conditions, we have developed the ReactorSTM system [16]. This system combines a small flow reactor, integrated with an STM into a UHV system that is equipped with standard, high-quality surface preparation and analysis techniques, such as ion bombardment, metal deposition, XPS, AES, and LEED. The architecture of the system is such that the sample can be transported from the various sample preparation and analysis tools into the ReactorSTM without breaking the UHV conditions. During the HP STM experiments, the UHV stays uncompromised even at pressures inside the reactor well above 1 bar. The flow-reactor geometry and the special design of the low-volume high-purity gas supply system allows us to continuously control the gas mixture composition in the reactor, the flow rate, and the reactor pressure, and it allows for rapid, time-resolved analysis on the gas effluent from the reactor during STM imaging, without the need to retract the tip, which would result in a 'blind moment'. In this way, this system enables us to study the surface structure of an active catalyst with atomic resolution, combined with simultaneous reactivity measurements. Thereby, we can directly correlate structural changes with chemical activity. The system is a strongly improved version of the prototype that we reported on earlier [3,11] and a commercial version has been developed by Leiden Probe Microscopy BV [17]. In this paper, we report on the first results from this new instrument applied to two different catalytic reactions, both on the Pt(1 1 0) surface: CO oxidation and NO reduction. CO oxidation is one of the reactions occurring in the catalytic cleaning of exhaust gases from automotive engines. Selective oxidation of CO to CO₂ has also received major attention in order to clean H₂ streams for fuel cells [18]. Typical catalysts used for this reaction include the noble metals, such as Pt [19]. The (1 1 0) surface of Pt is perhaps the best studied surface after Pt(1 1 1) for the oxidation of CO. Early studies of this reaction system have revealed highly interesting phenomena, such as, kinetic oscillations [20] and reaction induced faceting [21]. However, these phenomena were observed in a pressure range from high vacuum to UHV and using traditional surface science techniques. This experimental window in which detailed information of the surface can be obtained has been dramatically increased by the recent developments of *in situ* and *operando* techniques. Because of the interesting discoveries obtained in vacuum, it is easy to understand that this surface received much attention from researchers using these newly developed techniques. One of the key questions is whether the behavior observed under vacuum conditions can be extrapolated to real reaction conditions and which new surprises can be found on the other side of the pressure gap.

High-pressure STM [3] and SXRD combined with DFT [4] have revealed the appearance of new surface structures and compositions, depending on the gas composition. Two of these structures are oxidic in nature. One is a surface oxide probably stabilized by carbonate ions and oxygen atoms. This oxide is observed when the ratio between the partial pressures of CO and O₂ is not too low. The other oxidic structure is a thin film of bulk-like α -PtO₂ and is formed at lower CO to O₂ partial-pressure ratios. Interestingly, both oxides show a higher reactivity towards CO oxidation compared to the metallic surface. The formation of α -PtO₂ and the reactivity to CO has been confirmed by one ambient-pressure XPS study [22], while a second study at slightly different pressure and gas compositions compared to the STM and SXRD studies showed only the metallic surface [23]. In addition to the surface oxide observed by SXRD, a different structure has been observed in which O atoms bind to the FCC hollow sites of a reconstructed (1x2)-Pt(1 1 0) surface. In this surface oxide, the O-atom-induced stress leads to the ejection of Pt atoms in a highly ordered manner, so that a Pt(1 1 0)-(12x2)-220 structure is adopted [24]. However, DFT combined with *ab initio*

thermodynamics predicts that this surface oxide is not stable under reaction conditions [25,26].

The oxidation of CO by O₂ serves as a 'model system' to demonstrate the improved resolution of the ReactorSTM under catalytic conditions.

The second part of this work describes experiments on the interaction between NO and H₂ and the Pt(1 1 0) surface. These interactions are key factors in understanding the selective reduction of NO, which is an extremely important process to clean exhaust gases of engines and large turbines. In contrast to the oxidation of CO, there is hardly any *in situ* or *operando* result reported on the reduction of NO. Previous work from our group shows that results obtained under reaction conditions strongly differ from the results obtained in UHV on the reaction between NO and CO on Pt(1 0 0) [27]. On Pt(100), the surface switches between a (1x1) reconstruction and a quasi-hexagonal structure depending on the CO/NO ratio at 1.25 bar.

Different reducing agents can be used for this reaction, such as unburned fuel remains, CO and H₂. Hydrogen can be formed in exhaust gases by a water gas shift reaction (Eq. (1)) or via steam reforming with for example methane (Eq. (2)).



We continue this paper with a brief description of the ReactorSTM and the considerations with respect to purity and contaminations. After the experimental section, the results of the high-pressure, high-temperature study of CO oxidation on Pt(1 1 0) are described and discussed, followed by the structural changes observed on the same surface during high-pressure room temperature exposure to H₂ and NO.

2. Experimental

The results presented in this paper have all been obtained with the ReactorSTM [16] and establish the first scientific output of this unique system, which is an improved version of the HP STM described by Rasmussen et al. [11]. Herbschleb et al. describe the ReactorSTM in full detail elsewhere [16]. Therefore, we only summarize the most important features of the system. The ReactorSTM is a flow cell integrated within an STM inside a UHV system. Only a few parts of the STM are exposed to the reactive gases, *i.e.*, the tip and a slider that forms part of the STM's coarse approach mechanism. Most parts of the STM, such as the piezo tube, are outside the flow cell.

The combination between a UHV system and a flow cell gives the best of both worlds, fundamental surface science and the more applied catalytic research. We can use model catalysts and obtain a very clean and controlled starting point for the high-pressure experiment. Because we use a small flow reactor instead of back-filling a large-volume chamber, we can measure the reactivity with a much lower detection limit and higher time resolution. This reactivity is measured by leaking a small fraction of the gas from the reactor into a separate UHV chamber housing a Quadrupole Mass Spectrometer (QMS).

The Pt(1 1 0) sample, which was spark cut and polished to within 0.1° from the (1 1 0) plane [28], was cleaned with repetitive Ar⁺ sputtering and annealing in UHV at temperatures between 900 and 1100 K before every experiment. This procedure was complemented with an anneal step at 800 K in an oxygen atmosphere (1 × 10⁻⁸ – 1 × 10⁻⁷ mbar) to remove residual carbon. The removal of carbon and other impurities was checked with AES, until the peaks corresponding to impurities were on the level of the noise. In addition to the surface purity, LEED was used to determine the surface structure. The crystal was cleaned until LEED

showed a well-defined (1x2) reconstruction. This reconstruction, the missing-row reconstruction, is known to occur on the clean (110) surfaces of Ir, Au, and Pt under UHV conditions [29]. The well-known distances of 0.78 nm [30] between the missing rows of the clean Pt(110)-(1x2) surface in UHV have been used to calibrate the in-plane displacement of the piezo tube scanner of the STM. Monoatomic steps of the Pt(110) surface have been used to calibrate the vertical direction.

In order to start a high-pressure experiment, the sample must be transferred to the reactor. The sample itself forms the top wall of the reactor and is pressed onto the reactor body, which holds the STM tip and the electrical connection from the tip to the STM preamplifier. The sample is sealed on the reactor with a fluoroelastomer (Kalrez) o-ring, forming a high-pressure vacuum barrier that allows to maintain UHV conditions in the STM chamber and a pressure in the reactor of up to 6 bar. After the sample is pressed on the reactor, the reactor volume is no longer being pumped until the high-pressure gas flow is admitted. The pressure in the stage between UHV sample cleaning and the starting of the high-pressure experiment is solely determined by outgassing of the fluoroelastomer and other polymer parts, which is roughly estimated to be lower than 1×10^{-5} mbar. This outgassing is both temperature

and time dependent with possibly some memory effects occurring between experiments. However, careful baking of the entire reactor should minimize crosstalk between experiments.

Recently, we have implemented a new configuration in which two small pumping lines have been constructed to maintain some pumping of the reactor volume by the UHV chamber in the time lag between UHV and HP conditions. This improved configuration has been used for the NO and H₂ exposure experiments reported here. Before the STM experiment can start, a coarse approach needs to be employed to bring the tip within tunneling distance of the surface. Since there is no optical access to the STM when the reactor is closed this coarse approach must bridge a few millimeters and roughly takes between 20 and 60 minutes. To keep the sample as clean as possible one needs to question whether it is better to approach in a vacuum determined by outgassing and low pumping speed or to expose the sample directly to a flow of high-pressure inert gases. When flowing high pressure of a gas mixture, the contamination is limited by the impurity level in the gas feed. The used gases all have typical purities of 6.0N, which corresponds to an impurity level of 1 ppm. This impurity level corresponds to a partial pressure of 1×10^{-3} mbar at a total pressure of 1 bar. However, having a gas flow through the reactor has the advantage that partial pressures of impurities outgassing from the polymer components are reduced to lower levels.

To start a high-pressure experiment with a sample that resembles the well-prepared UHV sample as closely as possible, it was found that it was best to execute the coarse approach step before introducing the gas flow.

Mechanically cut PtIr tips have been used in the CO oxidation experiments without any *in situ* pretreatment. On the other hand, AC-etched (in aqueous solution of NaOH) W has been used as a tip in all the NO and H₂ exposure experiments. After introduction into the STM, the W-tip was sputtered with Ar⁺ to remove oxides and other contaminants from the apex of the tip. All STM images have been recorded from top left to bottom right with the fast scan direction from left to right and have been corrected with line-by-line background subtraction and have been analyzed and imaged using Gwyddion [31] and Spacetime [32].

3. Results and discussion

3.1. CO oxidation over Pt(110)

Figs. 1 and 2 summarize characteristic STM images obtained during CO oxidation experiments under high-pressure, high-temperature conditions. Fig. 1 shows three STM images of the Pt(110) surface under different reaction conditions. Fig. 1A (25 nm × 25 nm) shows the surface in vacuum at room temperature after being transferred to the reactor, and after the coarse approach of the tip. The surface clearly shows a pattern of rows. The distance between these rows is 0.75 ± 0.03 nm determined from the height profile shown in Fig. 1A, which is in excellent agreement with the theoretical value of the (1x2) missing-row reconstruction of 0.78 nm [30]. Interestingly, in the upper left part of the image the surface deviates from the missing-row pattern and small patches become apparent. At this point the surface has been exposed to poor vacuum, determined by the outgassing of the reactor walls and seals without being pumped for the time it takes to perform the approach of the tip. Therefore, we attribute the appearance of these patches to the partial lifting of the (1x2) missing-row reconstruction due to adsorption of outgassing molecules.

The sample was heated to 433 K and a flow of a mixture of CO and O₂ (CO/O₂ ratio >0.2) was introduced at a total pressure of 1 bar. Under these conditions, the (7.5 nm × 7.5 nm) STM image shown in Fig. 1B has been recorded. Excitingly, the high-pressure and elevated temperatures have not significantly deteriorated the imaging quality. The image clearly again shows a row pattern on the

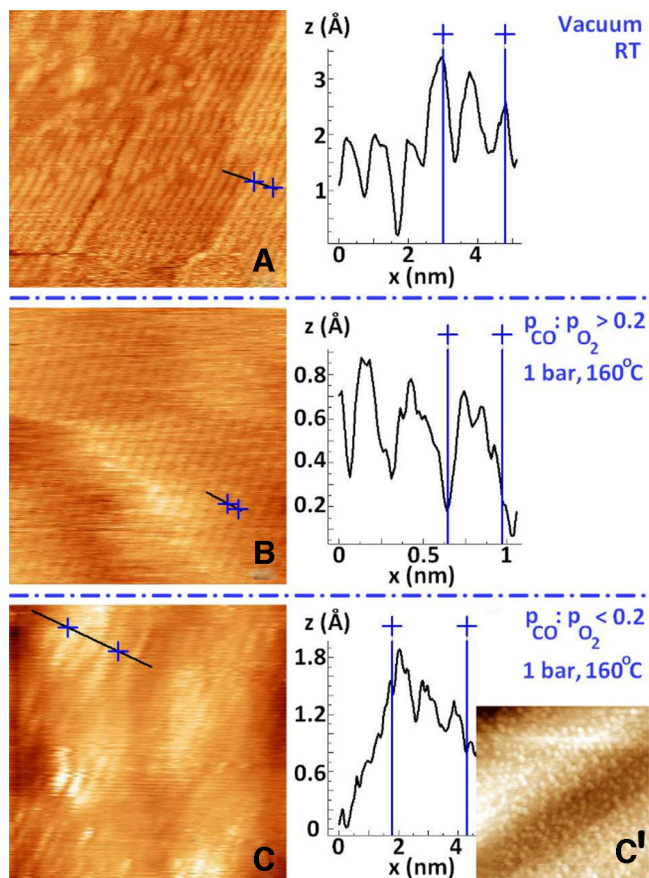


Fig. 1. STM images and corresponding height profiles obtained with the ReactorSTM during CO oxidation experiments under high-pressure, high-temperature conditions. (A), The missing-row reconstruction, room temperature, vacuum, 25 nm × 25 nm, $V_{\text{bias}} = 2.39$ V, and $I_{\text{tunnel}} = 49$ pA. Partial lifting of the reconstruction is observable in the top left of the image. (B), the unreconstructed (1x1) surface in CO-rich conditions, 1 bar, 433 K, 7.5 nm × 7.5 nm, $V_{\text{bias}} = -0.04$ V, and $I_{\text{tunnel}} = -86$ pA. (C), the (1x2) surface oxide in O₂ rich-conditions, 1 bar, 433 K, 12.5 nm × 12.5 nm, $V_{\text{bias}} = -0.10$ V, and $I_{\text{tunnel}} = -39$ pA. A few bad scan lines due to feedback instabilities have been removed to enhance the image quality. (C'), large scale image of the surface oxide, same conditions, 210 nm × 210 nm [3]. (C') shows the formation of protrusions on the surface as a result of the Mars-van Krevelen-like reaction mechanism.

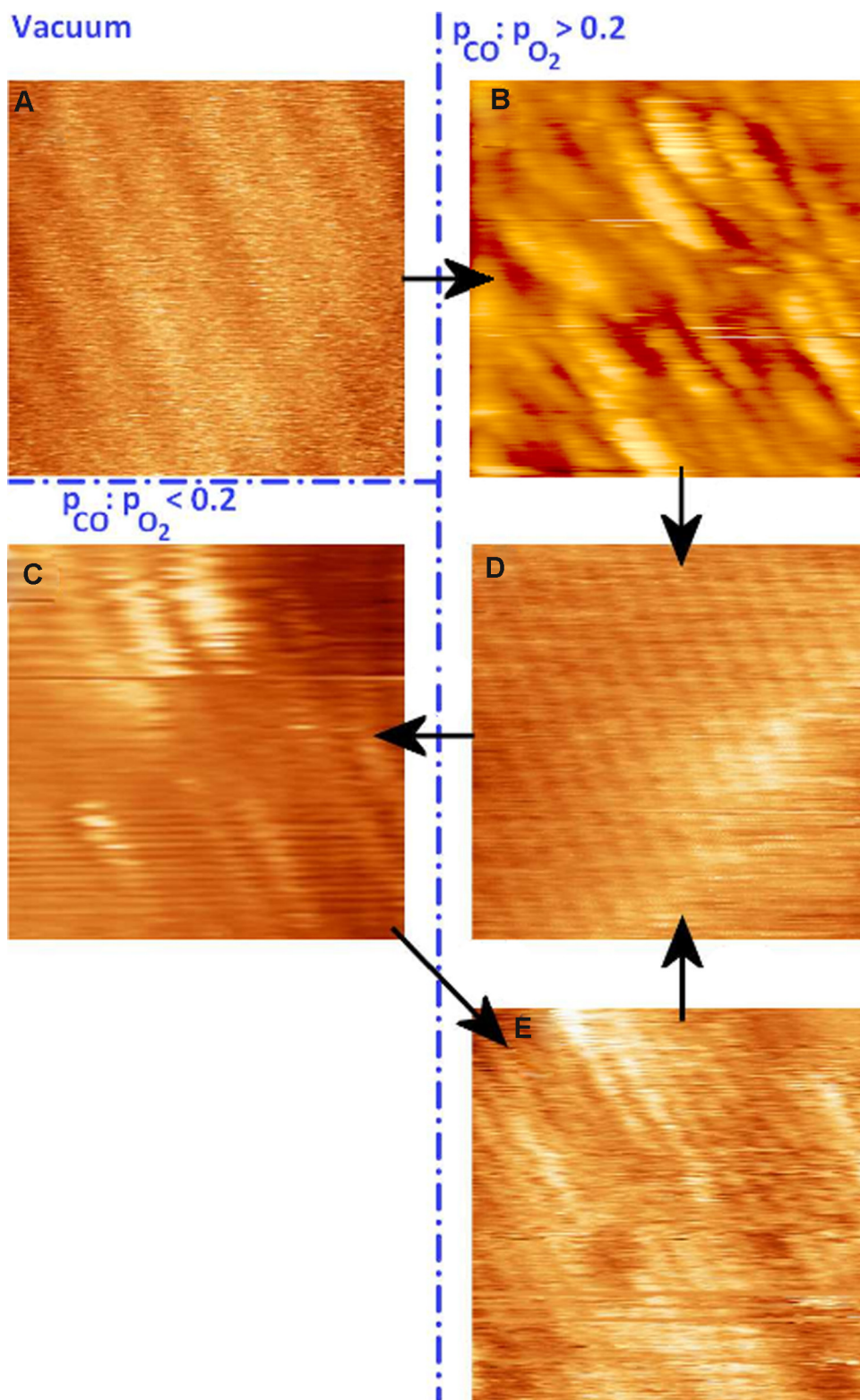


Fig. 2. STM images obtained with the ReactorSTM demonstrating the development of roughness at various stages of the CO oxidation experiment. (A), missing-row reconstruction, room temperature, vacuum, $4.5 \text{ nm} \times 4.5 \text{ nm}$, $V_{bias} = -0.10 \text{ V}$, and $I_{tunnel} = -52 \text{ pA}$. (B), lifting of the reconstruction observed during exposure to 1 bar of CO. Note that the transition from the missing-row reconstructed (1x2) surface to the (1x1) structure has made the surface rough. $T = 433 \text{ K}$, $15 \text{ nm} \times 15 \text{ nm}$, $V_{bias} = 0.10 \text{ V}$, and $I_{tunnel} = 749 \text{ pA}$. (C), flat (1x1) structure in a CO-rich flow, $T = 433 \text{ K}$, $4.5 \text{ nm} \times 4.5 \text{ nm}$, $V_{bias} = -0.04 \text{ V}$, and $I_{tunnel} = -86 \text{ pA}$. (D), commensurate (1x2) structure, observed immediately after switching to a more O_2 -rich gas mixture. Note that the surface is still relatively smooth. $T = 433 \text{ K}$, $4.5 \text{ nm} \times 4.5 \text{ nm}$. (E), Rough, metallic (1x1) surface, observed after increasing the CO content of the gas mixture again. $T = 433 \text{ K}$, $4.5 \text{ nm} \times 4.5 \text{ nm}$, $V_{bias} = 0.08 \text{ V}$, and $I_{tunnel} = -1004 \text{ pA}$.

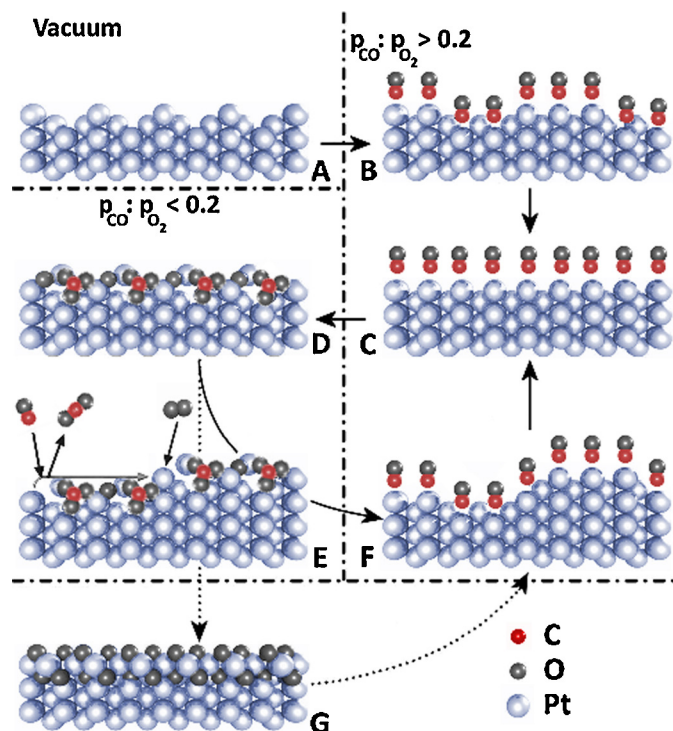


Fig. 3. A ball model explaining the different transitions observed in studying CO oxidation on Pt(110). (A) shows the missing-row reconstruction in vacuum. This reconstruction is lifted in CO-rich flow to give a rough (1x1) surface. (B). This roughened surface flattens out with time, (C). When the O₂ content is increased the commensurate lifted-row oxide is formed, (D). The Mars-van Krevelen-like reaction mechanism increases the roughness over time, (E). Increasing the CO partial pressure results in a rough (1x1) surface, (F), which smoothens over time, (C). At high O₂ partial pressures the incommensurate α -PtO₂ can be formed, (G).

two imaged terraces. The distance between these rows corresponds to the (1x1) unreconstructed surface, as can be read off from the height profile in Fig. 1B. This is the first time that the row structure of this surface has been observed under these reaction conditions. The blurry appearance of the step edge reflects the highly dynamic step fluctuations that are typical, given the high-temperature, high-pressure conditions. To summarize, the high-pressure exposure of the Pt(110) surface to a CO-rich flow lifts the (1x2) missing-row reconstruction and reveals a well-ordered (1x1) structure.

Fig. 1C shows the sample in an O₂-rich flow with a CO/O₂ ratio of less than 0.2. In this regime, the surface has switched again, this time to a row pattern with a row distance of 0.72 ± 0.06 nm, corresponding to a (1x2) structure. Remarkably, even with the roughness we observed under these conditions, the atomic rows are resolved and they exhibit the same row distance at all height levels.

This (1x2) structure is not a missing-row reconstruction. If it were, one should expect an abrupt increase in roughness, when the surface switches from the (1x1) to the (1x2) structure, since the top layer of Pt atoms in the (1x1) surface contains twice the number of Pt atoms compared to the top layer of the (1x2) missing-row reconstruction. As a result, one should expect that after the transition the surface would exhibit an island and hole pattern of two height levels. This transition-induced roughness would then decay over time. However, this behavior has not been observed. Instead, the opposite was witnessed. Immediately after the switch, there was no increase in roughness, whereas roughness was observed to build up as a function of time after the transition. Fig. 1C shows a stage in which significant roughness had been built up already, in the form of protrusions with a height of several nanometers. This increased roughness could be attributed to the catalytic reaction taking place under these conditions. Before discussing this

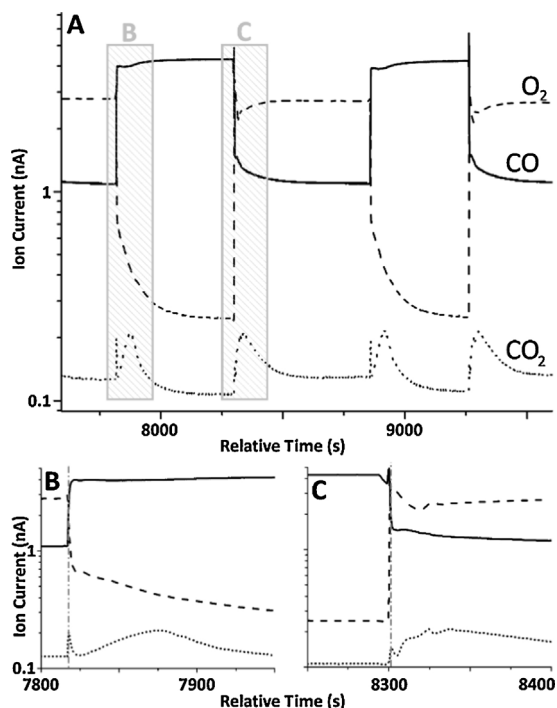


Fig. 4. Semi-logarithmic plot of the reaction kinetics during CO oxidation, measured with a QMS. The measured ion current is proportional to the partial pressure of the selected mass. (A), two cycles in which the gas composition has been changed back and forth from CO (solid line) to O₂ (dashed line) rich. The product of this reaction, CO₂ (dotted line) shows broad peaks during the switching between the gases that can be explained with LH kinetics. In the case of random adsorption, the maximum of each LH peak corresponds to a situation with equal O_{ad} and CO coverages. (B) and (C), grey dashed regions are replotted on an expanded time scale. The oxide shows higher activity (compare the tails in CO₂ between (C) and (B)). The spike in (B) indicates the high reaction rate on the oxide during the initial stage of increase of the CO partial pressure, followed by the drop in the rate, when the oxide is removed due to the high CO partial pressure.

mechanism in further detail, we present results of more experiments where we attempted to decouple both mechanisms (decay of the roughness introduced by lifting of the surface reconstruction vs. building up roughness due to the catalytic reactions). We prepared a clean Pt(110) surface, exposed it to a high-pressure CO flow in order to find the initial roughness that is associated with the lifting of the (1x2) missing-row reconstruction and the decay over time. The results of this experiment are shown in Fig. 2. Fig. 2A shows the initial (1x2) reconstructed Pt(110) surface, imaged in vacuum. After setting up the CO flow at 1 bar, we find initially increased roughness (Fig. 2B) which eventually decays, resulting in the flat (1x1) periodicity (Fig. 2C).

The experiment was continued by adding O₂ to the flow. The (1x1) surface shown in Fig. 2C changes to the (1x2) structure when the CO/O₂ ratio is decreased below 0.2 (O₂ rich mixture, Fig. 2D), which corresponds to the conditions of the measurement shown in Fig. 1C. Because the dimensions of 2C and 2D are identical, the images can be directly compared and the doubling of the distance between the rows is clearly observable. In Fig. 2D, there is no immediate increase in roughness, excluding the possibility that this structure reflects the formation of the missing-row reconstruction, as explained above. Prolonged exposure of the sample to O₂-rich conditions results in the increase of roughness over time, which is intimately related to catalytic turnover. This will be further discussed below. The result of this roughening is still present immediately after switching the flow back to CO-rich conditions and the accompanying transition from (1x2) back to (1x1). Under CO-rich

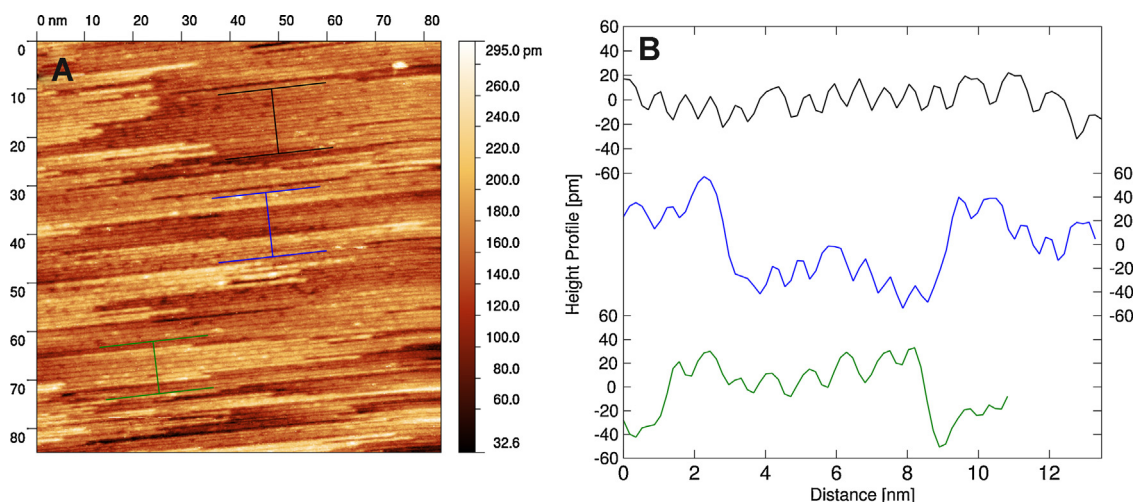


Fig. 5. (A), STM image, 84 nm \times 85 nm, $V_{bias} = -0.70$ V, and $I_{tunnel} = 121$ pA with, (B), three height profiles of Pt(110) obtained with the sample in the closed reactor in vacuum at room temperature prior to the NO reduction experiments.

conditions (Fig. 2E) the surface roughness decreases steadily over time to the level of Fig. 2C.

The nature of the (1x2) structure occurring under reaction conditions at CO/O₂ partial pressure ratios below 0.2 has been studied previously by STM [3], SXRD, and DFT [4]. The STM study suggested the structure to be an oxide, based on a change detected in the electronic structure inferred from Scanning Tunneling Spectroscopy. The SXRD study identified this structure under similar conditions to be a commensurate lifted-row reconstruction in which every second row is lifted, thus giving a (1x2) periodic structure. The lowest-energy structure with such lifted rows, found in DFT calculations, was stabilized by a combination of a row of carbonate ions below each lifted Pt row [4]. In addition to pushing the Pt row up, they also displace it sideways, in accordance with the SXRD analysis. In addition, the DFT results indicate the presence of a row of surface oxygen atoms bonding to each lifted Pt row. Combining the results of these studies, it is convincingly shown that this (1x2) structure formed under O₂-rich conditions is a commensurate oxide in which every second row is lifted by the incorporation of carbonate ions. Figs. 1C and 2D represent the first series of STM images in which this (1x2) lifted-row structure, which only appears under these harsh reaction conditions, is resolved in real space.

The increasing roughness under reaction conditions has been measured before on Pt(110) [3] and on Pd(100) [33,34], and is explained as a side effect of a Mars-Van-Krevelen-like reaction mechanism [35]. In this mechanism, the catalyst plays an even more intimate role than in other reaction mechanisms in heterogeneous catalysis. One of the reactants actually reacts with the catalyst to form a film of what could be regarded as an intermediate product in the reaction. Subsequently, the other reactant reacts with this intermediate product. In this model catalyst, we have identified the active structure of the catalyst under O₂-rich conditions to be a commensurate surface oxide, as explained above. The oxygen atoms from the oxide layer react with CO to form CO₂, leaving behind reduced and undercoordinated Pt atoms.

Pt atoms that become sufficiently undercoordinated, which probably requires the local loss of two or more oxygen atoms, may be expected to become mobile and diffuse over the surface. These Pt atoms will become immobilized again when they are oxidized by oxygen arriving from the gas phase. This reduction-diffusion-oxidation cycle will enhance the roughness of the surface.

When the CO/O₂ ratio is decreased even further, the hexagonal and incommensurate α -PtO₂ is formed on the surface, as observed with HP SXRD [4]. However, this α -PtO₂ has not been detected in

the ReactorSTM, most likely because the CO/O₂ partial pressure ratio could not be lowered far enough in this experiment.

A model summarizing the results of this work, previous STM data, the SXRD data, and the DFT results is given in Fig. 3. The well-prepared surface in vacuum shows the (1x2) missing-row reconstruction (Fig. 3A). This reconstruction is lifted in a CO-rich flow forming a rough (1x1) surface (Fig. 3B). The roughness is decreasing over time enhanced by the elevated temperature to a well-ordered (1x1) structure (Fig. 3C). When the composition is changed from CO to O₂ rich, the commensurate surface oxide forms, with the incorporated carbonate ions (Fig. 3D). The roughness of this oxide increases as a result of the Mars-Van Krevelen-like reaction mechanism (Fig. 3E). Increasing the CO concentration again reduces the oxide and a rough (1x1) surface is obtained (Fig. 3F). The rough (1x1) surface smoothens to restore a flat (1x1) surface as depicted in Fig. 3C. The cycle between Figs. 3C, 3D, 3E, and 3F could be reproduced many times. A parallel cycle involves the formations of the incommensurate and bulk-like α -PtO₂ at an even lower CO/O₂ ratio. This oxide also roughens through a similar mechanism, only much slowly because the reaction rate is lower due to the low concentration of CO present. As mentioned already, this α -PtO₂ has not yet been observed in the ReactorSTM.

One of the major advantages of the ReactorSTM over other STMs able to scan at near-ambient pressures is that we can not only go to higher pressures and temperatures, but also measure the reaction kinetics simultaneously with imaging the surface. The kinetic results for the present study of CO oxidation are presented in Fig. 4. The most obvious features in Fig. 4 are the broad peaks in the CO₂

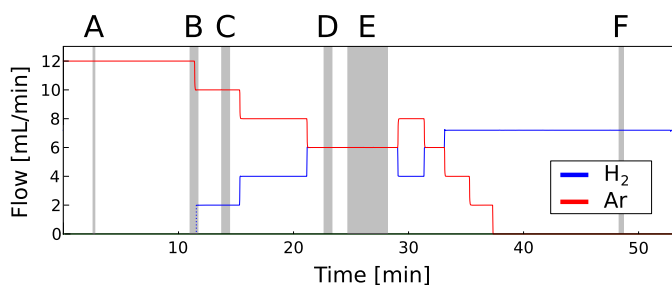


Fig. 6. Change in gas composition measured as a function of Ar (red) and H₂ (blue) flow rates. The pressure inside the reactor was kept constant at 1.2 bar throughout the entire sequence. Note that the total flow rate (sum of Ar and H₂ flow rates) was varied. The grey regions indicate the time intervals in which the STM images of Figs. 7A–F were obtained.

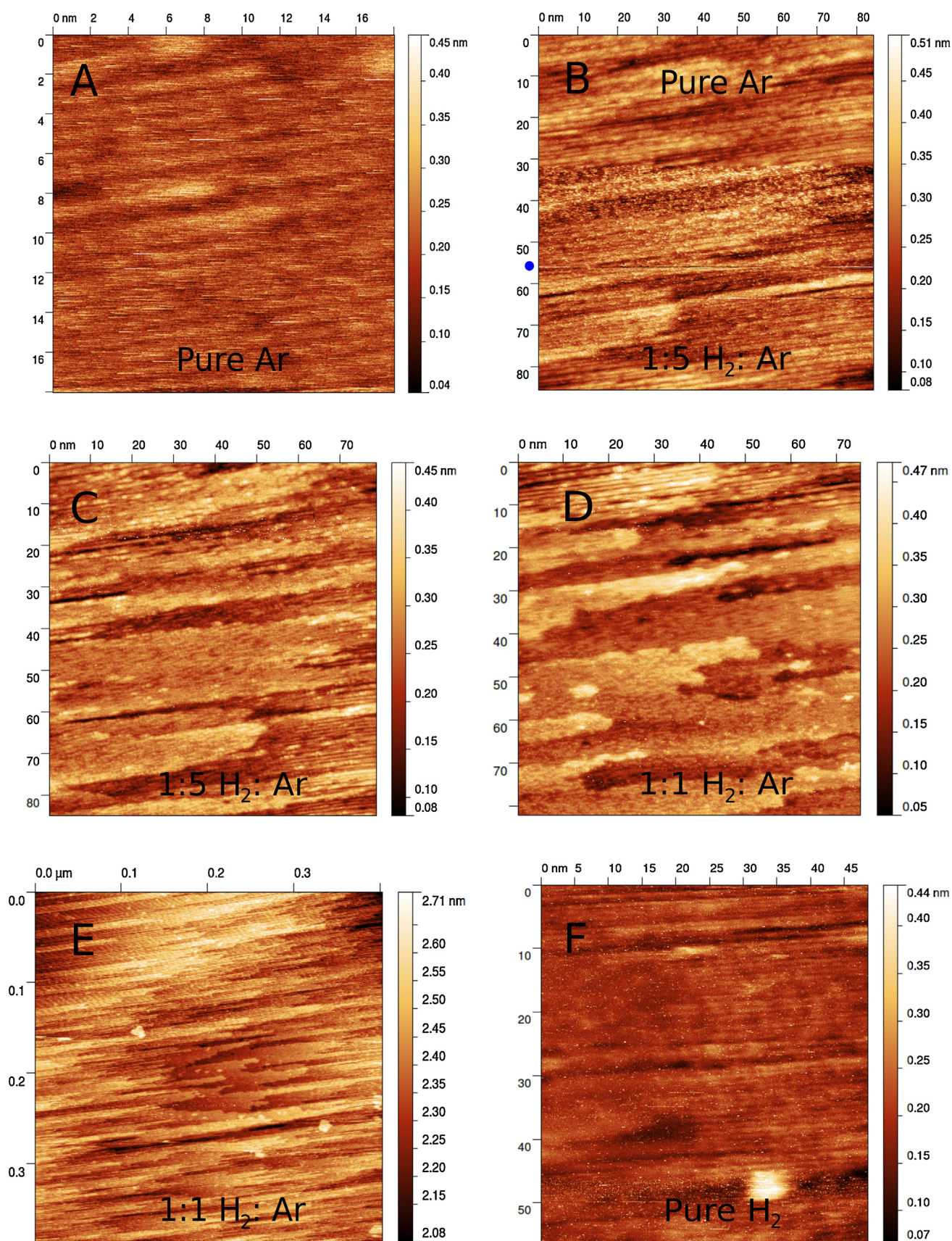


Fig. 7. STM images obtained with the ReactorSTM during exposure of Pt(1 1 0) at room temperature to mixtures of Ar and H₂. The STM images were measured from top to bottom. (A), Surface imaged in pure Ar, 18 nm × 18 nm, $I_{\text{tunnel}} = 60$ pA. (B), STM image during switch from pure Ar to 1:5 H₂/Ar ratio. The blue dot indicates the scan line of the switch. 84 nm × 85 nm, $I_{\text{tunnel}} = 98$ pA. (C), 1:5 H₂/Ar ratio, 79 nm × 85 nm, $I_{\text{tunnel}} = 165$ pA. (D), 1:1 H₂/Ar ratio, 75 nm × 82 nm, $I_{\text{tunnel}} = 165$ pA. (E), 1:1 H₂/Ar ratio, 403 nm × 386 nm, $I_{\text{tunnel}} = 165$ pA. (F), pure H₂, 49 nm × 56 nm, $I_{\text{tunnel}} = 166$ pA. All STM images were obtained at room temperature and with $V_{\text{bias}} = -0.70$ V.

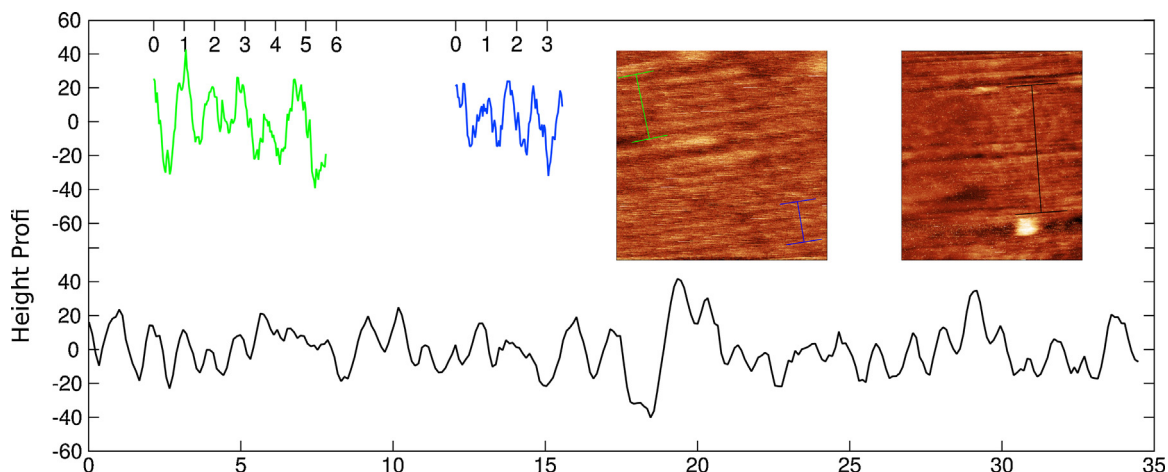


Fig. 8. Three height profiles averaged around zero. Two height profiles (green and blue) were taken from Fig. 7A and one (black) from 7F. The inset shows the STM images with the projection of these height profiles.

production, when switching back and forth from CO to O₂ rich. These peaks are indicative of Langmuir–Hinshelwood (LH) kinetics in which the reactivity is highest when the CO and O surface coverages are equal. The details in Fig. 4, however, show more interesting behavior. One is the fact that the reactivity of the oxide, which is present under oxygen rich conditions, is higher than the reactivity of the metallic surface, which is present under CO-rich conditions. The other interesting detail is the presence of narrow spikes notable just before the LH peaks in the CO₂ production but only when switching from the oxide to the metallic surface. These spikes are ascribed to the increase in reaction rate when the CO content above the oxide is raised and the sudden drop in reaction when the active surface oxide is removed at the point where the CO supply has become too high. To make this effect more visible, Figs. 4B and 4C show two small regions of Fig. 4A on an expanded time scale.

3.2. Exposure to H₂ and NO

The second reaction that we investigate in this article, is the reduction of NO by H₂ on Pt(1 1 0). This reaction is related to the reduction of NO by CO, which is again one of the important reactions in an automotive catalyst. The nature of this system is more complicated than the oxidation of CO, in which there is only one major reaction with a single product. To reduce NO using H₂ several pathways are possible, creating a combination of NH₃, H₂O and N₂, among others. These products could have a profound influence on the structure of the catalyst. The first stage in our investigation of this reaction system has been to expose Pt(1 1 0) to H₂ and NO at high pressure (1.2 bar) at room temperature.

In these experiments, the starting configuration of the Pt(1 1 0) surface was less well-ordered than that in the CO oxidation experiments, presented in Figs. 1A and 2A. In Fig. 5A, an STM image of 84 nm × 85 nm is shown. Before this image was measured, the surface was exposed for several minutes to the poor vacuum of the flow reactor cell. In the STM image, it is clearly visible that the surface shows a pattern of rows with a few distinct widths, which we will discuss first.

Fig. 5B shows three height profiles taken from Fig. 5A. These height profiles have been averaged over several lines to increase the signal-to-noise ratio. Profile 1 (black) shows predominantly narrow rows with a repeat distance of 0.74 nm. This measured distance corresponds nicely to the (1×2) period of 0.78 nm [30]. In this height profile, several larger periods can be observed of 1.14 nm. The height corrugation of these wider rows is somewhat larger

than that for the rows with the regular (1×2) period. The increase in both width and corrugation suggest that the wider periods are (1×3) missing-row configurations. Profile 2 and 3 (blue and green) in Fig. 5B also show mixtures of the (1×2) and (1×3) structures and mono-atomic steps on the Pt(1 1 0) surface. Partial lifting as observed in Fig. 1A has not been witnessed in the low vacuum of the reactor before the NO reduction experiments. This change with respect to the CO oxidation experiments can be attributed to the increased pumping speed of the reactor before starting the high-pressure experiments. In conclusion, the Pt(1 1 0) at the start of the NO reduction experiment showed a mixed (1×2) and (1×3) missing-row structures without the partial lifting of the surface reconstruction.

3.2.1. HP exposure to Ar-H₂ at RT

After the surface had been characterized in the reactor vacuum, a flow of Ar was established at a pressure of 1.2 bar. After setting this flow, the surface was imaged within a minute. After 10 minutes in the Ar flow, the gas composition was changed stepwise from pure Ar to pure H₂ while the surface was imaged with STM. The change of gas composition over time was realized within 30 minutes and is depicted in Fig. 6. Figs. 7A and 7F show STM images of the surface in pure Ar and pure H₂, respectively. When these images are compared to the image of Fig. 5A taken in vacuum, an increase in noise is apparent at the higher pressure. This increase could be the result of impurities in the Ar flow that interact with the tip. Nevertheless, we still resolve the atomic rows. In addition to atomic steps, rows within the terraces can be observed.

In Figs. 7B–E, four STM images are shown for intermediate H₂/Ar gas compositions. Fig. 7B shows the image in which the gas composition was changed from pure Ar to 1:5 H₂/Ar ratio. Due to the gas-flow-induced change in the vertical drift, the height signal of the STM shows precisely at which point in time the surface was confronted with the change in gas composition (see blue dot in Fig. 7B). This effect remains visible even after line-by-line background subtraction. It is noteworthy that before the gas switch a tip change occurred in pure Ar. This tip change greatly enhanced the resolution and some additional internal structure became visible within the atom rows. Figs. 7D and 7E show STM images for higher H₂/Ar ratios. The images show a progressive rounding of the steps and a gradual disordering of the missing-row structure. Fig. 7E is an image that was zoomed out with respect to Fig. 7D. A mild, rectangular depression can be discerned in the center of Fig. 7E, corresponding to the scan area of Fig. 7D and previous STM images. The structure that is visible in this region seems somewhat

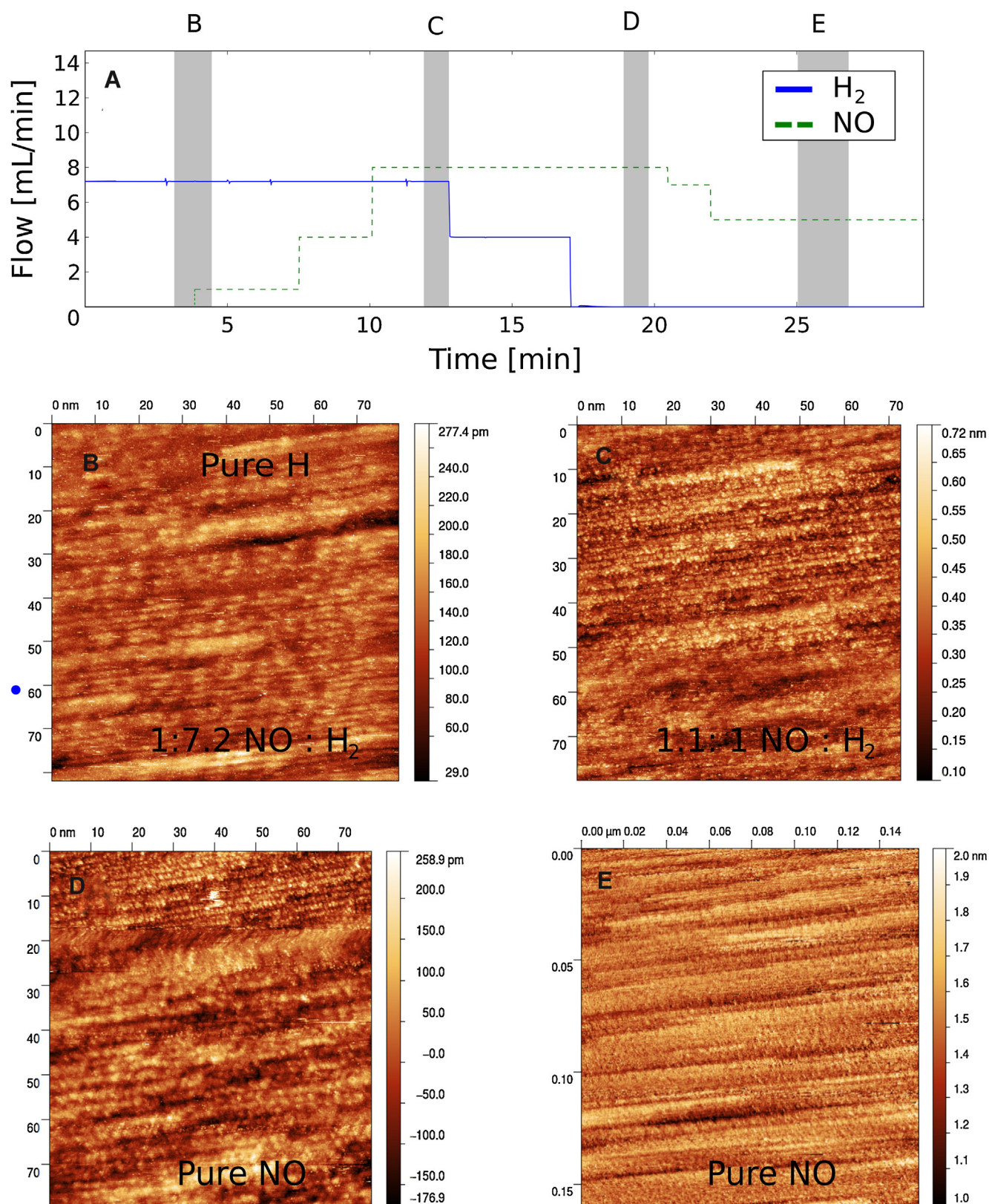


Fig. 9. Gas composition as a function of time and *in situ* STM data. (A) shows the stepwise change from H₂ (blue, flow in mL/min) to NO (green, flow set point in mL/min) at room temperature at a constant reactor pressure of 1.2 bar. Grey regions indicate at which point in time and conditions the four, (B–E), STM images were obtained. (B), surface imaged in pure H₂, 80 nm × 82 nm, $I_{\text{tunnel}} = 139$ pA. (C), surface in nearly equal H₂/NO ratio, 73 nm × 80 nm, $I_{\text{tunnel}} = 141$ pA. (D), sample in pure NO atmosphere, 78 nm × 80 nm, $I_{\text{tunnel}} = 141$ pA. (E), surface after prolonged NO exposure, 158 nm × 160 nm, $I_{\text{tunnel}} = 139$ pA. All STM images were obtained with $V_{\text{bias}} = -0.70$ V. STM images recorded in NO flow show frequent tip changes to a state with strongly enhanced resolution.

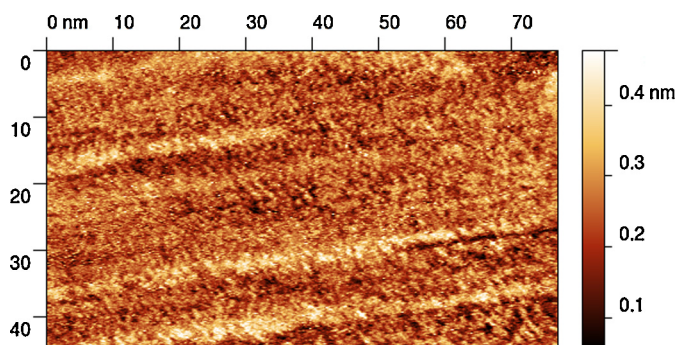


Fig. 10. Enlarged view of selected region out of an STM images measured in a pure NO flow at room temperature showing enhanced resolution after a tip change. $77 \text{ nm} \times 45 \text{ nm}$, $V_{\text{bias}} = -0.70 \text{ V}$ and $I_{\text{tunnel}} = 140 \text{ pA}$.

smoother than that in the freshly scanned region around it. This smooth depression is probably tip-induced and may be indicative of tip-enhanced surface mobility under these conditions. To separate between changes induced by the gas composition and to minimize tip effects, Fig. 7F was taken in a completely fresh region of the surface. Fig. 8 shows height profiles taken from Figs. 7A and 7F, which are reproduced in the insets. Two height profiles (green and blue, Fig. 8) have been taken from the image in pure Ar (Fig. 7A), and they predominantly show a regular row pattern. The period correspond to the (1x2) missing-row structure with isolated larger periods, most likely (1x3) missing-row configurations, similar to the structure observed in vacuum (Fig. 5).

The black curve in Fig. 8 shows the height profile of the image taken in pure H_2 . This height line shows structures with both the (1x2) and the (1x3) missing-row periods as well. The observation that both missing-row structures remain intact indicates that the exposure to Ar and (short) exposure to H_2 does not significantly change the surface structure.

3.2.2. HP exposure to H_2 -NO at RT

Prolonged exposure of the Pt(110) surface (48 minutes after H_2 was first introduced) to H_2 at 1.2 bar at RT, resulted a row structure with a (1x4) rows, identified to have a (1x4) periodicity. Also, some deeper missing rows can be observed (Fig. 9B). A detailed analysis of this (1x4) structure and the conditions under which it forms will be the subject of a separate paper [36]. The (1x4) reconstructed surface has been exposed to NO at increasing NO/ H_2 ratios, see Figs. 9C–E. Fig. 9A shows the gas composition as a function of time. During each change of gas composition, the surface was continuously imaged. The blue dot in the first image indicates the switching point from pure H_2 to an NO/ H_2 ratio of 0.14. In general, the imaging quality seems to deteriorate only slightly when switching from H_2 to the more reactive NO. This observation is rather remarkable since the material of the tip was W and this is not known as a particularly noble metal. Tip changes are visible in Figs. 9C and 9D, some of which temporarily enhance the imaging resolution significantly. Features of one to several pixels can be distinguished with very high contrast. In both images a single pixel corresponds to 0.21 nm, slightly smaller than the distance between neighboring Pt atoms (0.277 nm [37]). Fig. 10 shows a selected region from an STM image taken directly before Fig. 9E in a pure NO atmosphere. This region exhibit enhanced resolution and the row structures can be seen to have disappeared. Directly after the acquisition of this image, the scan region was zoomed out a factor two to check for tip effects, see Fig. 9E. Although the resolution in Fig. 9E is not as high as that in Fig. 10, no tip effect is identified and the loss of the row structure is observed to have occurred also outside of the previously scanned area.

Figs. 9 and 10 demonstrate that when surface and tip are exposed to a gas flow that contains NO, frequent tip changes occur that often lead to a significant improvement in imaging resolution. This effect could be caused by the adsorption of NO on the tip apex, thereby changing the tunneling characteristics. Functionalizing STM tips to improve resolution or to give chemical contrast in STM images has been achieved before with CO [38,39], S [40], H_2 [41], and O_2 [42].

Currently, We are investigating the H_2 - and NO-induced structural changes of the Pt(110) surface at elevated temperatures, which appear to be more dramatic than the rearrangements reported here for room temperature. These higher-temperature observations are complemented with measurements of the reaction rates, e.g., by measuring the partial pressure of the N_2 that is produced, as we illustrated in Fig. 4 for the CO oxidation reaction on the same surface. These higher-temperature experiments will form the subject of a future publication.

4. Conclusions

In this paper, we have presented the first results obtained with the ReactorSTM, an STM combined with a flow reactor cell. This system was used to study two highly interesting catalytic reaction systems, namely CO oxidation and NO reduction, both on the Pt(110) surface. Under CO oxidation conditions, we have shown that this surface can adopt different structures. The (1x2) missing-row reconstruction exhibited by a clean Pt(110) surface, is lifted under reaction conditions. At high CO partial pressure, the surface shows an unreconstructed Pt(110)-(1x1) structure. At lower CO/ O_2 partial pressure ratios, the surface transforms into a (1x2) surface oxide. Previous STM, SXRD and DFT studies have identified this oxide as a lifted-row configuration, stabilized by the incorporation of rows of carbonate ions and oxygen atoms [4]. In this paper, we have presented the first STM images, in which the atomic rows of this structure are resolved. In addition to this strong dependence of the surface structure on the partial pressures of the reactants, we measured an increased catalytic activity of the surface oxide compared to the metallic (1x1) surface. This higher activity reflects an alternative reaction pathway of the Mars-Van-Krevelen type. We have also observed that this reaction leads to the build-up of surface roughness. The α - PtO_2 structure, that we have identified with SXRD under even more O_2 -rich conditions was not observed in the present STM study, possibly because the CO/ O_2 partial pressure ratio has not reached sufficiently low values in this experiment.

To acquire more insight into the reduction of NO, another important reaction in heterogeneous catalysis, we have studied the structural changes of the Pt(110) surface as a function of NO and H_2 partial pressure. Prolonged H_2 exposure produced both a (1x4) missing-row configuration and some deeper nested missing rows. NO exposure of this surface slowly lifted the surface reconstruction and the row pattern disappeared, leaving flat terraces on the surface. Remarkably, the W tip was relatively stable in the corrosive NO atmosphere. Even more interestingly, the tip frequently switched into a state with significantly improved imaging resolution under NO-rich conditions.

Acknowledgements

This work is supported by NanoNextNL, a micro and nanotechnology consortium of the Government of the Netherlands and 130 partners.

Furthermore, this project was financially supported by a Netherlands SmartMix grant and the NIMIC partner organizations through NIMIC, a public-private program.

References

- [1] M. Bowker, *The Basis and Applications of Heterogeneous Catalysis*, Oxford Chemistry Primers, 1998.
- [2] G.A. Somorjai, *Introduction to Surface Chemistry and Catalysis*, Wiley, New York, 1993.
- [3] B.L.M. Hendriksen, J.W.M. Frenken, CO oxidation on Pt(110): scanning tunneling microscopy inside a high-pressure flow reactor, *Phys. Rev. Lett.* 89 (2002) 046101, <http://dx.doi.org/10.1103/PhysRevLett.89.046101>.
- [4] M.D. Ackermann, T.M. Pedersen, B.L.M. Hendriksen, O. Robach, S.C. Bobaru, I. Popa, C. Quiros, H. Kim, B. Hammer, S. Ferrer, J.W.M. Frenken, Structure and reactivity of surface oxides on Pt(110) during catalytic CO oxidation, *Phys. Rev. Lett.* 95 (2005) 25505.
- [5] X. Su, P.S. Cremer, Y.R. Shen, G.A. Somorjai, High-pressure CO oxidation on Pt(111) monitored with infrared-visible sum frequency generation (SFG), *J. Am. Chem. Soc.* 119 (1997) 3994.
- [6] R. Westerström, J. Gustafson, A. Resta, A. Mikkelsen, J.N. Andersen, E. Lundgren, N. Seriani, F. Mittendorfer, M. Schmid, J. Klikovits, P. Varga, M.D. Ackermann, J.W.M. Frenken, N. Kasper, A. Stierle, Oxidation of Pd(553): from ultrahigh vacuum to atmospheric pressure, *Phys. Rev. B* 76 (2007) 155410, <http://dx.doi.org/10.1103/PhysRevB.76.155410>.
- [7] H. Over, M. Muhler, Catalytic CO oxidation over ruthenium-bridging the pressure gap, *Prog. Surf. Sci.* 72 (2003) 3.
- [8] B.L. Weeks, C. Durkan, H. Kuramochi, M.E. Welland, T. Rayment, A high pressure, high temperature, scanning tunneling microscope for in situ studies of catalysis, *Rev. Sci. Instrum.* 71 (2000) 3777, <http://dx.doi.org/10.1063/1.1290043>.
- [9] J.F. Creemer, S. Helveg, G.H. Hovelings, S. Ullmann, A.M. Molenbroek, P.M. Sarro, H.W. Zandbergen, Atomic-scale electron microscopy at ambient pressure, *Ultramicroscopy* 108 (2008) 993, <http://dx.doi.org/10.1016/j.ultramic.2008.04.014>.
- [10] R. van Rijn, M.D. Ackermann, O. Balmes, T. Dufrane, A. Geluk, H. Gonzalez, H. Isern, E. de Kuyper, L. Petit, V.A. Sole, D. Wermeille, R. Felici, J.W.M. Frenken, Ultrahigh vacuum/high-pressure flow reactor for surface x-ray diffraction and grazing incidence small angle x-ray scattering studies close to conditions for industrial catalysis, *Rev. Sci. Instrum.* 81 (2010) 014101, <http://dx.doi.org/10.1063/1.3290420>.
- [11] P.B. Rasmussen, B.L.M. Hendriksen, H. Zeijlemaker, H.G. Ficke, J.W.M. Frenken, The "Reactor STM": A scanning tunneling microscope for investigation of catalytic surfaces at semi-industrial reaction conditions, *Rev. Sci. Instrum.* 69 (1998) 3879, <http://dx.doi.org/10.1063/1.1149193>.
- [12] F. Tao, D. Tang, M. Salmeron, G.A. Somorjai, A new scanning tunneling microscope reactor used for high-pressure and high-temperature catalysis studies, *Rev. Sci. Instrum.* 79 (2008) 084101.
- [13] S.B. Roobol, M.E. Cañas-Ventura, M. Bergman, M.A. van Spronsen, W.G. Onderwaater, P.C. van der Tuijn, R. Koehler, A. Oifitserov, G.J.C. van Baarle, J.W.M. Frenken, The ReactorAFM: Non-Contact Atomic Force Microscope operating under high-pressure and high-temperature catalytic conditions, 2014, in preparation.
- [14] L. Kuipers, R.W.M. Loos, H. Neerings, J. ter Horst, G.J. Ruwiel, A.P. de Jongh, J.W.M. Frenken, Design and performance of a high-temperature, high-speed scanning tunneling microscope, *Rev. Sci. Instrum.* 66 (1995) 4557, <http://dx.doi.org/10.1063/1.1145289>.
- [15] M.S. Hoogeman, D.G. van Loon, R.W.M. Loos, H.G. Ficke, E. de Haas, J.J. van der Linden, H. Zeijlemaker, L. Kuipers, M.F. Chang, M.A.J. Klik, J.W.M. Frenken, Design and performance of a programmable-temperature scanning tunneling microscope, *Rev. Sci. Instrum.* 69 (1998) 2072, <http://dx.doi.org/10.1063/1.1148901>.
- [16] C.T. Herbschleb, P.C. van der Tuijn, S.B. Roobol, V. Navarro, J.W. Bakker, Q. Liu, D. Stoltz, M.E. Cañas-Ventura, G. Verdoes, M.A. van Spronsen, M. Bergman, L. Crama, I. Taminiu, A. Oifitserov, G.J.C. van Baarle, J.W.M. Frenken, The ReactorSTM: Atomically resolved scanning tunneling microscopy under high-pressure, high-temperature catalytic reaction conditions, *Rev. Sci. Instrum.* 85 (2014) 083703, <http://dx.doi.org/10.1063/1.4891811>.
- [17] Leiden Probe Microscopy BV, <http://www.leidenprobemicroscopy.com/>
- [18] S.H. Oh, R.M. Sinkevitch, Carbon Monoxide Removal from Hydrogen-Rich Fuel Cell Feedstreams by Selective Catalytic Oxidation, *J. Catal.* 142 (1993) 254, <http://dx.doi.org/10.1006/jcat.1993.1205>.
- [19] C.T. Campbell, G. Ertl, H. Kuipers, J. Segner, A molecular beam study of the catalytic oxidation of CO on a Pt(111) surface, *J. Chem. Phys.* 73 (1980) 5862, <http://dx.doi.org/10.1063/1.440029>.
- [20] M. Eiswirth, G. Ertl, Kinetic oscillations in the catalytic CO oxidation on a Pt(110) surface, *Surf. Sci.* 177 (1986) 90, [http://dx.doi.org/10.1016/0039-6028\(86\)90259-1](http://dx.doi.org/10.1016/0039-6028(86)90259-1).
- [21] S. Ladas, R. Imbihl, G. Ertl, Microfacetting of a Pt(110) surface during catalytic CO oxidation, *Surf. Sci.* 197 (1988) 153, [http://dx.doi.org/10.1016/0039-6028\(88\)90578-X](http://dx.doi.org/10.1016/0039-6028(88)90578-X).
- [22] D.R. Butcher, M.E. Grass, Z. Zeng, F. Aksoy, H. Bluhm, W.X. Li, B.S. Mun, G.A. Somorjai, L. Zhi, In situ oxidation study of Pt(110) and its interaction with CO, *J. Am. Chem. Soc.* 133 (2011) 20319.
- [23] J.Y. Chung, F. Aksoy, M.E. Grass, H. Kondoh, P. Ross Jr., L.Z.B.D. Mun, In situ study of the catalytic oxidation of CO on a Pt(110) surface using ambient pressure X-ray photoelectron spectroscopy, *Surf. Sci.* 603 (2009) L35.
- [24] W.X. Li, L. Österlund, E.K. Vestergaard, R.T. Vang, J. Matthiesen, T.M. Pedersen, E. Lægsgaard, B. Hammer, F. Besenbacher, Oxidation of Pt(110), *Phys. Rev. Lett.* 93 (2004) 146104-1.
- [25] T.M. Pedersen, W.X. Li, B. Hammer, Structure and activity of oxidized Pt(110) and α -PtO₂, *Phys. Chem. Chem. Phys.* 8 (2006) 1566.
- [26] T. Zhu, S.G. Sun, R.A. van Santen, E.J.M. Hensen, Reconstruction of Clean and Oxygen-Covered Pt(110) Surfaces, *J. Phys. Chem. C* 117 (2013) 11251.
- [27] C.T. Herbschleb, S.C. Bobaru, J.W.M. Frenken, High-pressure STM study of NO reduction by CO on Pt(100), *Catal. Today* 154 (2010) 61, <http://dx.doi.org/10.1016/j.cattod.2010.03.029>.
- [28] Surface Preparation Laboratory Zaandam, the Netherlands, <http://www.spl.eu/>
- [29] K.M. Ho, K.P. Bohnen, Stability of the missing-row reconstruction on fcc (110) transition-metal surfaces, *Phys. Rev. Lett.* 59 (1987) 1833, <http://dx.doi.org/10.1103/PhysRevLett.59.1833>.
- [30] E. Vlieg, I.K. Robinson, K. Kern, Relaxations in the missing-row structure of the (1x2) reconstructed surfaces of Au(110) and Pt(110), *Surf. Sci.* 233 (1990) 248, [http://dx.doi.org/10.1016/0039-6028\(90\)90636-M](http://dx.doi.org/10.1016/0039-6028(90)90636-M).
- [31] D. Nečas, P. Klapetek, Gwyddion: an open-source software for SPM data analysis, *Cent. Eur. J. Phys.* 10 (2012) 181, <http://dx.doi.org/10.2478/s11534-011-0096-2>.
- [32] S.B. Roobol, J.W.M. Frenken, Spacetime: analysis software for microscopy data of dynamical processes, in: in Preparation, 2014.
- [33] B.L.M. Hendriksen, S.C. Bobaru, J.W.M. Frenken, Oscillatory CO oxidation on Pd(100) studied with in situ scanning tunneling microscopy, *Surf. Sci.* 552 (2004) 229, <http://dx.doi.org/10.1016/j.susc.2004.01.025>.
- [34] R. van Rijn, O. Balmes, A. Resta, D. Wermeille, R. Westerström, J. Gustafson, R. Felici, E. Lundgren, J.W.M. Frenken, Surface structure and reactivity of Pd(100) during CO oxidation near ambient pressures, *Phys. Chem. Chem. Phys.* 13 (2011) 13167, <http://dx.doi.org/10.1039/C1CP20989B>.
- [35] P. Mars, D.W. van Krevelen, Oxidations carried out by means of vanadium oxide catalysts, in: the Proceedings of the Conference on Oxidation Processes, *Chem. Eng. Sci.* 3 (Supplement 1) (1954) 41, [http://dx.doi.org/10.1016/S0009-2509\(54\)80005-4](http://dx.doi.org/10.1016/S0009-2509(54)80005-4).
- [36] M.A. van Spronsen, J.W.M. Frenken, I.M.N. Groot, Hydrogen induced (1x4) reconstruction, investigated by UHV STM, HP STM and HP SXRD, in Preparation (2014).
- [37] J.W. Arblaster, Crystallographic properties of platinum, *Platinum Metals Rev.* 41 (1997) 12–21.
- [38] L. Bartels, G. Meyer, K.H. Rieder, Controlled vertical manipulation of single CO molecules with the scanning tunneling microscope: a route to chemical contrast, *Appl. Phys. Lett.* 71 (1997) 213, <http://dx.doi.org/10.1063/1.119503>.
- [39] L. Gross, N. Moll, F. Mohn, A. Curioni, G. Meyer, F. Hanke, M. Persson, High-resolution molecular orbital imaging using a p-Wave STM Tip, *Phys. Rev. Lett.* 107 (2011) 086101, <http://dx.doi.org/10.1103/PhysRevLett.107.086101>.
- [40] Q.M. Xu, L.J. Wan, S.X. Yin, C. Wang, C.L. Bai, Effect of chemically modified tips on STM imaging of 1-octadecanethiol molecule, *J. Phys. Chem. B* 105 (2001) 10465, <http://dx.doi.org/10.1021/jp011916a>.
- [41] R. Temirov, S. Soubatch, O. Neucheva, A.C. Lassise, F.S. Tautz, A novel method achieving ultra-high geometrical resolution in scanning tunnelling microscopy, *New J. Phys.* 10 (2008) 053012 <http://stacks.iop.org/1367-2630/10/i=5/a=053012>
- [42] Z. Cheng, S. Du, W. Guo, L. Gao, Z. Deng, N. Jiang, H. Guo, H. Tang, H.-J. Gao, Direct imaging of molecular orbitals of metal phthalocyanines on metal surfaces with an O₂-functionalized tip of a scanning tunneling microscope, *Nano Res.* 4 (2011) 523, <http://dx.doi.org/10.1007/s12274-011-0108-y>.